# Endothelial-to-mesenchymal transition: a precursor to pulmonary arterial remodelling in patients with idiopathic pulmonary fibrosis

Archana Vijay Gaikwad[1,2], Wenying Lu [1,2,3], Surajit Dey[1], Prem Bhattarai[1], Greg Haug[1,4], Josie Larby[1,4], Collin Chia[1,3,4], Jade Jaffar [5,6], Glen Westall[5,6], Gurpreet Kaur Singhera[7,8], Tillie-Louise Hackett[7,8], Mathew Suji Eapen [1,2,9] and Sukhwinder Singh Sohal[1,3,9]

[1]Respiratory Translational Research Group, Department of Laboratory Medicine, School of Health Sciences, College of Health and Medicine, University of Tasmania, Launceston, TAS, Australia. [2]National Health and Medical Research Council Centre of Research Excellence in Pulmonary Fibrosis, Respiratory Medicine and Sleep Unit, Royal Prince Alfred Hospital, Camperdown, NSW, Australia. [3]Launceston Respiratory and Sleep Centre, Launceston, TAS, Australia. [4]Department of Respiratory Medicine, Launceston General Hospital, Launceston, TAS, Australia. [5]Department of Allergy, Immunology and Respiratory Medicine, The Alfred Hospital, Melbourne, VIC, Australia. [6]Department of Immunology and Pathology, Monash University, Melbourne, VIC, Australia. [7]Department of Anaesthesiology, Pharmacology and Therapeutics, University of British Columbia, Vancouver, BC, Canada. [8]Centre for Heart Lung Innovation, St Paul's Hospital, Vancouver, BC, Canada. [9]These authors contributed equally to this work.

Corresponding author: Sukhwinder Singh Sohal (sukhwinder.sohal@utas.edu.au)

Shareable abstract (@ERSpublications)
**EndMT is an active process in patients with IPF, and contributes to pulmonary arterial remodelling and fibrosis. This work also informs the early origins of pulmonary hypertension in patients with IPF. EndMT is a novel therapeutic target in IPF.** https://bit.ly/3Hof1pZ

**Cite this article as:** Gaikwad AV, Lu W, Dey S, *et al*. Endothelial-to-mesenchymal transition: a precursor to pulmonary arterial remodelling in patients with idiopathic pulmonary fibrosis. *ERJ Open Res* 2023; 9: 00487-2022 [DOI: 10.1183/23120541.00487-2022].



Received: 3 Oct 2022
Accepted: 26 Jan 2023

## Abstract

*Background* We have previously reported arterial remodelling in patients with idiopathic pulmonary fibrosis (IPF) and suggested that endothelial-to-mesenchymal transition (EndMT) might be central to these changes. This study aims to provide evidence for active EndMT in IPF patients.

*Methods* Lung resections from 13 patients with IPF and 15 normal controls (NCs) were immunostained for EndMT biomarkers: vascular endothelial cadherin (VE-cadherin), neural cadherin (N-cadherin), S100A4 and vimentin. Pulmonary arteries were analysed for EndMT markers by using computer- and microscope-assisted image analysis software Image ProPlus7.0. All the analysis was done with observer blinded to subject and diagnosis.

*Results* Increased expression of mesenchymal markers N-cadherin ($p<0.0001$), vimentin ($p<0.0001$) and S100A4 ($p<0.05$) was noted with downregulation of junctional endothelial VE-cadherin ($p<0.01$) in the intimal layer of the arteries from patients with IPF compared to NCs. Cadherin switch was observed in IPF patients, showing increase in endothelial N-cadherin and decrease in VE-cadherin ($p<0.01$). There was also VE-cadherin shift from junctions to cytoplasm ($p<0.01$), effecting endothelial cell integrity in patients with IPF. In IPF, individual mesenchymal markers vimentin and N-cadherin negatively correlated with diffusing capacity of the lungs for carbon monoxide ($r'= -0.63$, $p=0.03$ and $r'= -0.66$, $p=0.01$). Further, N-cadherin positively correlated with arterial thickness ($r'=0.58$, $p=0.03$).

*Conclusion* This is the first study to demonstrate active EndMT in size-based classified pulmonary arteries from IPF patients and potential role in driving remodelling changes. The mesenchymal markers had a negative impact on the diffusing capacity of the lungs for carbon monoxide. This work also informs early origins of pulmonary hypertension in patients with IPF.

## Introduction

Idiopathic pulmonary fibrosis (IPF) is a highly progressive lung disease with limited therapeutic options [1]. The current IPF pathophysiology emphasises the critical role of alveolar epithelial injury, followed by an

aberrant wound healing process resulting in fibrosis and destructive lung scarring, although the causes are unknown [1, 2]. Fibrosis of the lung restricts efficient gas exchange, effectively inducing systemic hypoxic conditions and death due to oxygen deficiency. Similar to the epithelial injury, alterations to pulmonary vasculature also occur, resulting in abnormal vascular remodelling [3]. The modification to the vascular structure includes proliferative intima, thickening of the medial smooth muscle layer, plexiform lesions and complete occlusion or narrowing of the vessels by scarred tissues [1, 3–5]. Such vascular remodelling can lead to pulmonary hypertension (PH), a comorbidity that frequently complicates IPF pathology and worsens prognosis, especially in late stages of the disease [6, 7].

Recent findings suggest the active involvement of several cells in IPF. However, cells vulnerable to transition under pathological conditions, such as airway basal epithelial cells, alveolar type II pneumocytes, macrophages and pulmonary endothelial cells, are crucial contributors to tissue fibrosis [8, 9]. The transition of endothelium occurs through endothelial-to-mesenchymal transition (EndMT), which is a critical mechanism in vascular remodelling that can further progress to fibrotic alterations [10–12]. EndMT-induced vascular changes are reported in IPF [1, 13, 14], intestinal fibrosis [15] and cardiac fibrosis [16]. Our recent study has found that arterial wall thickening, luminal occlusion and disruptive extracellular matrix (ECM) deposition occurs in IPF patients, and EndMT possibly drives these changes [3]. However, the contribution of EndMT to vascular remodelling and its association with lung fibrosis in IPF patients is poorly defined. In EndMT, loss of junctional proteins such as vascular endothelial cadherins (VE-cadherins) and gain of migratory mesenchymal traits occur. The increase in endothelial expression of mesenchymal proteins such as neural cadherin (N-cadherin), S100A4 and vimentin are suggestive of EndMT [17, 18].

This study investigates EndMT as a dynamic process in relation to vascular remodelling in IPF by analysing the EndMT biomarkers. We performed a quantitative assessment of endothelial junctional marker VE-cadherin and mesenchymal markers S100A4, vimentin and N-cadherin protein levels in the classified pulmonary arteries from patients with IPF and compared them with NCs. Furthermore, we analysed the correlations between the mesenchymal markers, arterial remodelling and lung function parameters.

## Material and methods

### *Study population*

Surgically resected human lung tissues from 13 patients with IPF were obtained from Alfred Health Biobank Melbourne (ethics ID: 336-13). None of the patients was on any antifibrotic medication, and all had pathologist-verified histopathology reports of usual interstitial pneumonia. Lung tissue specimens from 15 healthy normal control (NC) subjects, comprising small airways and parenchymal areas (ethics ID: H00-50110), were provided by the James Hogg Lung Registry, University of British Columbia. Detailed subject demographics are provided in table 1.

**TABLE 1** Subject demographics and clinical characteristics

| Factor | Normal control (NC) | IPF |
|---|---|---|
| **Total number n** | 15 | 13 |
| **Age years** | 44±20.1 | 64±5.06 |
| **Sex (F/M) n** | 6/5 | 6/7 |
| **Body mass index kg·m$^{-2}$** | NA | 26.69±3.03 |
| **Smoking status: (current smoker/ex-smoker/never-smoker) n** | Nonsmokers | 0/7/6 |
| **Smoking pack-years** | | 20.84±23.16 |
| **Lung physiology** | | |
| $FEV_1$ L | | 1.70 ±0.40 |
| $FEV_1$ % predicted | | 60.17±12.22 |
| FVC L | | 1.97±0.51 |
| FVC % predicted | | 53.5±12.98 |
| $D_{LCO}$ mmol·min$^{-1}$·kPa$^{-1}$ | | 5.91±2.92 |
| $D_{LCO}$ corrected % predicted | | 25.85±15.30 |

Data presented as mean±SD unless otherwise indicated. NA: not available; IPF: idiopathic pulmonary fibrosis; $FEV_1$: forced expiratory volume in 1 s; FVC: forced vital capacity; $D_{LCO}$: diffusing capacity of the lung for carbon monoxide.

### *Immunohistochemical staining for EndMT markers*

The lung tissue resections were deparaffinised using xylene and ethanol following antigen retrieval using a Decloaking Chamber (Biocare Medical, Pacheco, CA, USA) at 110°C for 15 min with target retrieval citrate buffer pH 6.0 (Dako S2369) and at 95°C for 15 min with retrieval buffer pH 9.0 (Dako S2367), respectively. The tissues were stained with EndMT primary antibodies, polyclonal rabbit anti-human S100A4 (1:1000; Dako A5114), VE-cadherin (CD144) mouse monoclonal (1:150; Thermofisher 14144982), vimentin mouse monoclonal (1:200; Dako M7020) and mouse monoclonal anti-N-cadherin (1:100; Abcam Ab98952) for 60 min; with inflammatory markers, including mouse anti-human CD4 (1:50, Dako M7310), mouse anti-human CD8 (1:50, Leica Biosystems, NCL-CD8-4B11-L-CE), CD68 (1:100, Dako M0814), mouse anti-human neutrophil elastase (1:200, Dako M0752) and mouse monoclonal mast cell chymase (CMA1, 1:100, Abcam ab2377); and with the pericyte marker platelet-derived growth factor receptor-β (PDGFR-β, 1:100, LSBio, LS-C150026); followed by secondary HRP rabbit/mouse antibodies (Dako K5007). The protein markers were visualised as brown with the addition of DAB substrate (Dako K5007). The nucleus was counterstained with haematoxylin (Australian Biostain P/L).

### *Measurement strategies for pulmonary arteries*

Arterial images were acquired from NCs and patients with IPF by using a 4× objective in a vertical uni-direction to avoid overlap. We used a Leica DM 500 microscope with attached Leica IC50W digital camera for analysis. Using measuring tools from the ProPlus 7.0 program, the external length (from one end to the other end of the adventitia) for pulmonary arteries was measured. These measurements were used for arterial classification into six groups: 100–1000 µm (interspaced 100 or 200 µm), similar to the strategy used in our earlier study [3].

### *VE-cadherin and N-cadherin expression in the basement membrane of pulmonary arteries*

We used different magnifications to capture images across all arterial sizes. For example, for smaller arteries measuring 100–199 µm a 63× objective, for 200–399 µm and 400–599 µm a 40× objective and for larger arteries 600–1000 µm a 20× objective was used. Further, for arterial size and subject, five images were randomly selected using an online random number generator for both VE-cadherin and N-cadherin. Firstly, two trace lines were drawn using the imaging software, one at the basement membrane and another one at the outer endothelium as the reference. The mean distance between the trace lines was calculated for basement membrane length using the automated program of tissue image analysis software Image-Pro Plus v7. Further, cells which stained positive (brown colour) for junctional and cytoplasmic VE-cadherin in the reference basement membrane area were counted (supplementary figure S1a). Likewise, cells which stained positive (brown colour) for junctional and cytoplasmic N-cadherin in the reference basement membrane area were counted (supplementary figure S1b). Additionally, total cells in the basement membrane were counted using the imaging software.[1]

VE-cadherin junctional and cytoplasmic positive cell percentage per average basement membrane was calculated using the following formula:

$$\text{VE-cadherin junctional or cytoplasmic positive cell percentage} = \left(\frac{\text{Number of positive expression cells}}{\text{Average length of basment membrane}}\right) \times 100$$

Similarly, N-cadherin junctional and cytoplasmic positive cell percentage per average basement membrane was calculated using the following formula:

$$\text{N-cadherin junctional or cytoplasmic positive cell percentage} = \left(\frac{\text{Number of positive expression cells}}{\text{Average length of basment membrane}}\right) \times 100$$

### *Pulmonary total arterial layer expression for vimentin, N-cadherin and S100A4*

Image acquisition and randomisation were followed in the same way as VE-cadherin and N-cadherin cell percentage measurements. For total arterial expression for each mesenchymal marker (vimentin, N-cadherin and S100A4 expression), an area of interest (AOI) from the start of the outer end of the intima facing the lumen to the outer border of adventitia was manually selected using imaging software. Subsequently, mesenchymal staining colour (brown) and total dark objects from the AOI were counted

using image ProPlus 7.0 software. A similar strategy was used for individual layers of intima, media and adventitia. For intimal layer mesenchymal marker expression, the outer luminal to the inner elastin layer was selected as the AOI, while for the medial mesenchymal marker expressions the external outline of the inner elastin membrane and internal lining of the external elastin membrane of the atrial smooth muscle layer was considered. The areas bordering the external elastin to the arteries' outermost connective tissue were considered as adventitia for the mesenchymal marker expression measurements (supplementary figure S1c). Percentage of vimentin, N-cadherin and S100A4 expression was calculated using the following formula:

$$\text{Each layer \% of mesenchymal marker expression} = \left(\frac{\text{Number of selected colour objects from AOI}}{\text{Total number of dark objects from AOI}}\right) \times 100$$

### *Correlations between the mesenchymal marker expression and vascular remodelling changes*

Our group has previously published the study on morphometric assessment of vascular remodelling changes observed among IPF patients [3, 19]. Here, we used same morphometric assessment data for correlation purposes since the patient's cohort was same. The correlation between each mesenchymal marker expression and arterial remodelling changes was calculated to understand the impact of EndMT.

### *Statistical analysis*

All cross-sectional data were tested for their normal distributions using the D'Agostino–Pearson omnibus normality test. Analysis of variance was performed with ordinary one-way ANOVA using Bonferroni multiple comparison tests, which compared mean and standard deviation across all groups of interest; specific group differences with correction for multiple comparisons were assessed using Dunn's test. Finally, for correlations, we performed regression analyses using Spearman's rank correlation test. All analysis was done using GraphPad prismV9, with a p-value $\leqslant 0.05$ being considered significant.

## Results

The pulmonary arteries from IPF patients exhibited notable morphological changes such as endothelial proliferation penetrating the lumen, muscular hypertrophy both in intima and medial layers and plexiform lesions compared to arteries from NCs. Cytoplasmic endothelial cell expression was observed for VE-cadherin in tissue sections from patients with IPF, while junctional expression was observed in NCs (figure 1a). Across all arterial sizes, mesenchymal protein N-cadherin expression was observed in all layers of classified arteries in IPF but was not seen in NCs (figure 1b). Strong vimentin and S100A4 staining were seen in all layers in IPF compared to NCs. Vimentin expression was predominantly observed in the smaller and medium-sized arteries (figure 1c). S100A4 staining was predominantly seen in the intima compared to media and adventitia across all arterial ranges in IPF patients. Comparatively there was less S100A4 staining than vimentin and less N-cadherin expression across all arterial sizes in IPF (figure 1d).

### *Endothelial VE-cadherin and N-cadherin cellular expression in IPF*

We assessed differential counts for VE- and N-cadherin in the junction and compared them with VE- and N-cadherin cytoplasmic expression, which is presented here as the percentage of total cells in the intimal area. Endothelium of NCs on average consisted of 40–50% cells that expressed junctional VE-cadherin, which drastically reduced to 5–15% in IPF ($p<0.01$), regardless of the arterial size (figure 2a (a) and b). In addition to the loss of junctional VE-cadherin in IPF patients, we also found an incremental increase in cytoplasmic VE-cadherin, which was fivefold that of cytoplasmic VE-cadherin in NCs across all arterial sizes ($p<0.01$) (figure 2a (b) and b (b)). A larger difference in cytoplasmic VE-cadherin in IPF and NCs was particularly noted for smaller arteries (range 100–199 µm) ($p<0.001$) compared to larger arteries. Interestingly, we also identified close to a twofold increase in junctional expression of N-cadherin cells across all arterial sizes ($p<0.05$) in IPF (figure 2a (c) and b (a)), although the cytoplasmic N-cadherin was only noticeable in IPF patients and was negligible in NCs (figure 2a (d) and b (b)).

### *Per cent N-cadherin expression in IPF*

There was a significant increase in N-cadherin expression across all arterial sizes in IPF compared to NCs. Total N-cadherin expression was considerably greater (four- to fivefold) in IPF compared to NCs across all arterial sizes ($p<0.0001$) (figure 3a). Furthermore, intimal and medial N-cadherin % expression revealed a greater fold change compared to that in the adventitial layer across the entire arterial range in IPF (figure 3b, c, d and e). We found that intimal and medial N-cadherin % expression was significantly higher across all classified arterial ranges, *i.e.*, 100–1000 µm ($p<0.0001$) in IPF (figure 3b, c, d and e). It was greatest in the 200–399 µm and 400–599 µm ($p<0.001$) (figure 3c, d) compared to the 100–199 µm ($p<0.01$) and 600–1000 µm ($p<0.05$) arterial range (figure 3b, e).

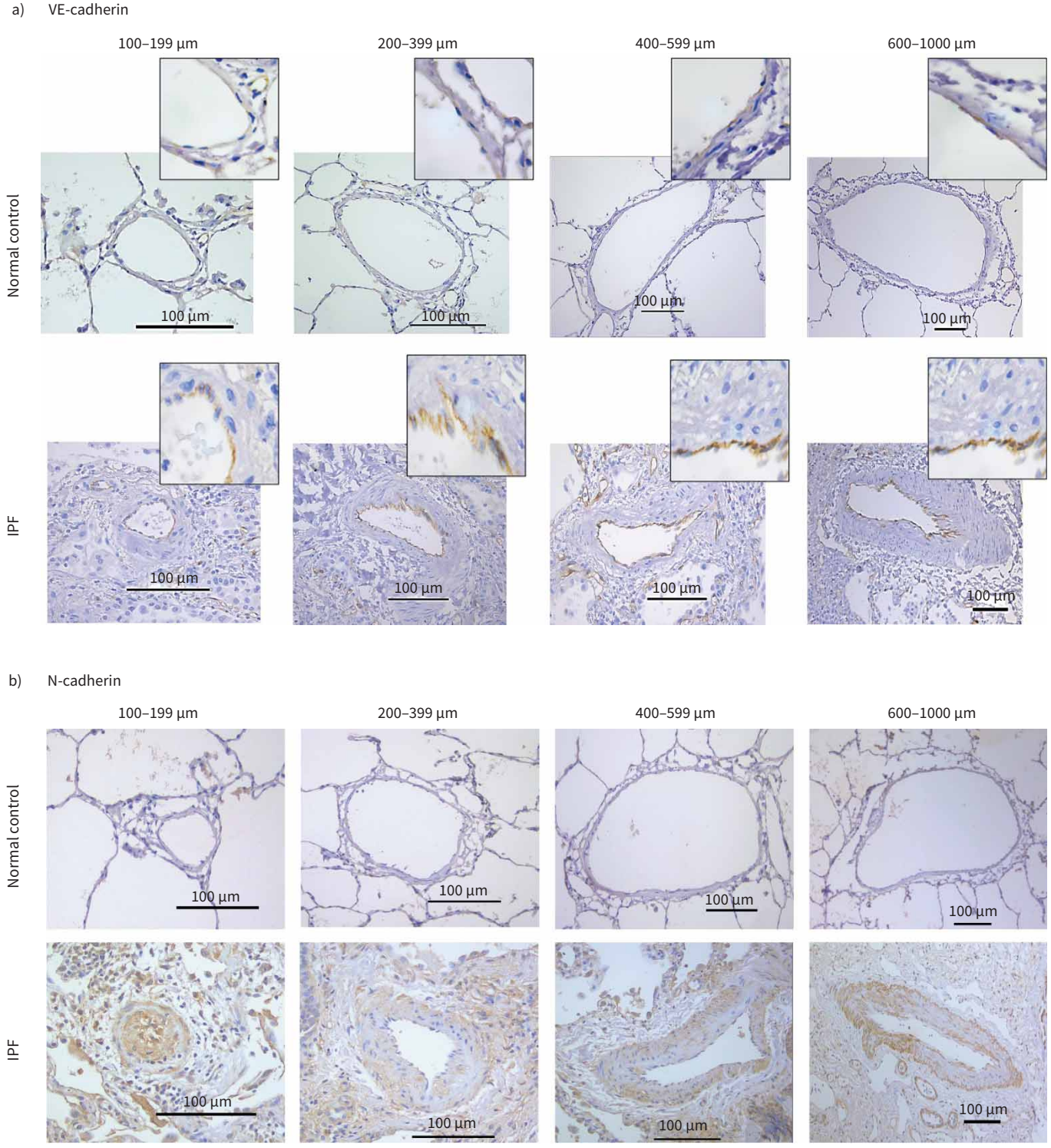


**FIGURE 1** a) Slides from normal control (NC) and idiopathic pulmonary fibrosis (IPF) patients of pulmonary arteries immunostained for VE-cadherin measuring 100–199 µm (20× magnification), 200–399 µm (20× magnification), 400–599 µm (20× magnification) and 600–1000 µm (10× magnification). b) Slides from normal control (NC) and idiopathic pulmonary fibrosis (IPF) patients of pulmonary arteries immunostained for N-cadherin measuring 100–199 µm (20× magnification), 200–399 µm (20× magnification), 400–599 µm (20× magnification) and 600–1000 µm (10× magnification). c) Slides from normal control (NC) and idiopathic pulmonary fibrosis (IPF) patients of pulmonary arteries immunostained for vimentin measuring 100–199 µm (20× magnification), 200–399 µm (20× magnification), 400–599 µm (20× magnification) and 600–1000 µm (10× magnification). d) Slides from normal control (NC) and idiopathic pulmonary fibrosis (IPF) patients of pulmonary arteries immunostained for S100A4 measuring 100–199 µm (20× magnification), 200–399 µm (20× magnification), 400–599 µm (20× magnification) and 600–1000 µm (10× magnification).

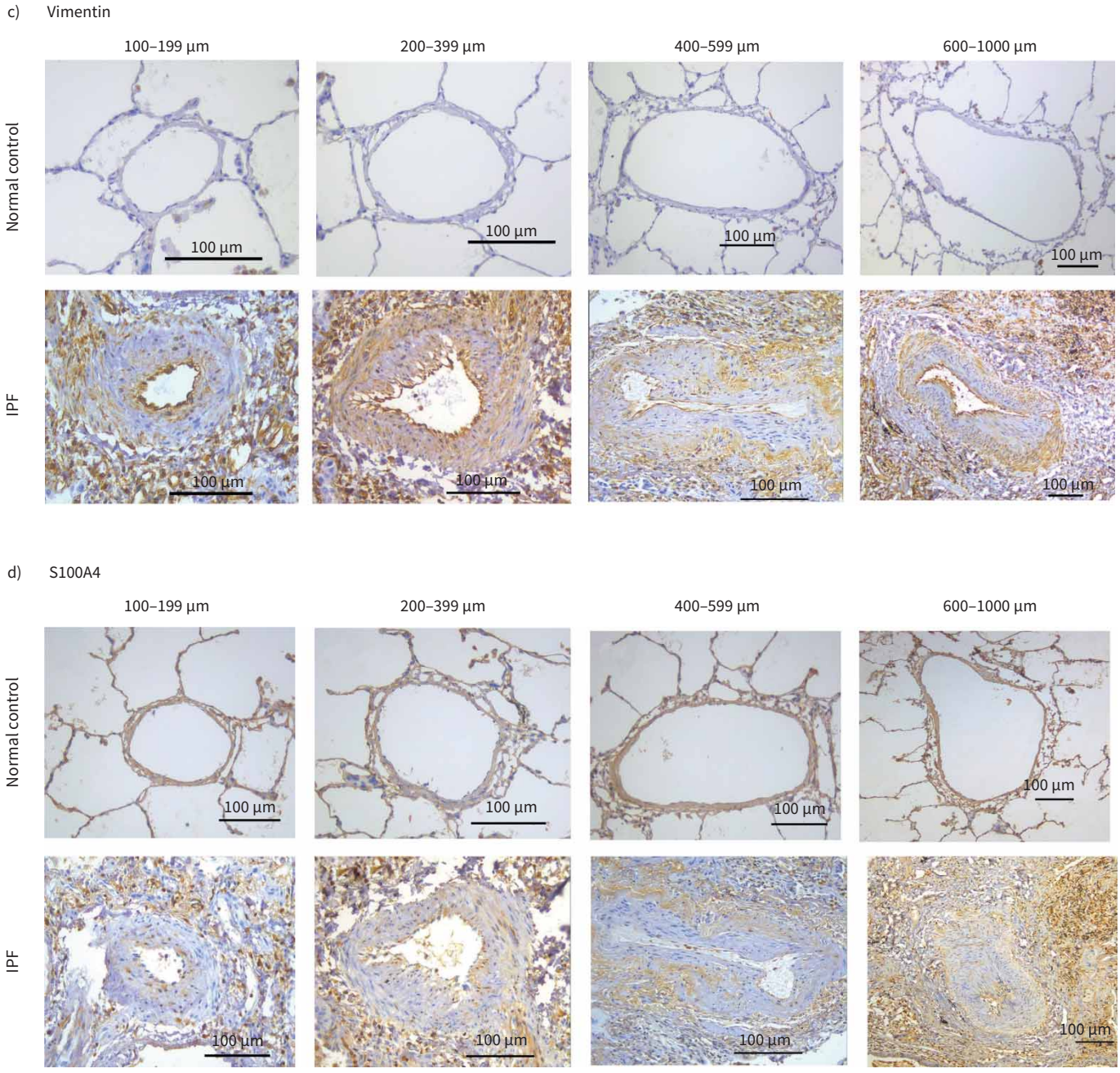


FIGURE 1 Continued.

### *Vimentin % expression in IPF*

The total vimentin percentage significantly increased throughout the arterial ranges in IPF compared to NCs ($p<0.0001$) (figure 4a). Vimentin expression in intima and media was significantly higher across all classified arterial ranges, *i.e.*, 100–1000 µm ($p<0.0001$) in IPF (figure 4b, c, d and e). Increase in vimentin expression was also noted in the adventitial layer for all arterial sizes. This was highly significant for the arterial range of 200–599 µm ($p<0.001$) (figure 4b, c, d, e).

### *S100a4 % expression in IPF*

Compared to NC, total percentage of staining for S100A4 was significantly higher in smaller and medium-sized arteries in IPF (100–199 µm ($p<0.0001$) and 200–399 µm ($p<0.001$)) (figure 5a). However, in larger arteries S100A4 expression was slightly higher in IPF (10–15%) compared to NCs (8–10%) (figure 5d and e). Intimal expression was significantly higher in smaller arteries measuring 199 µm

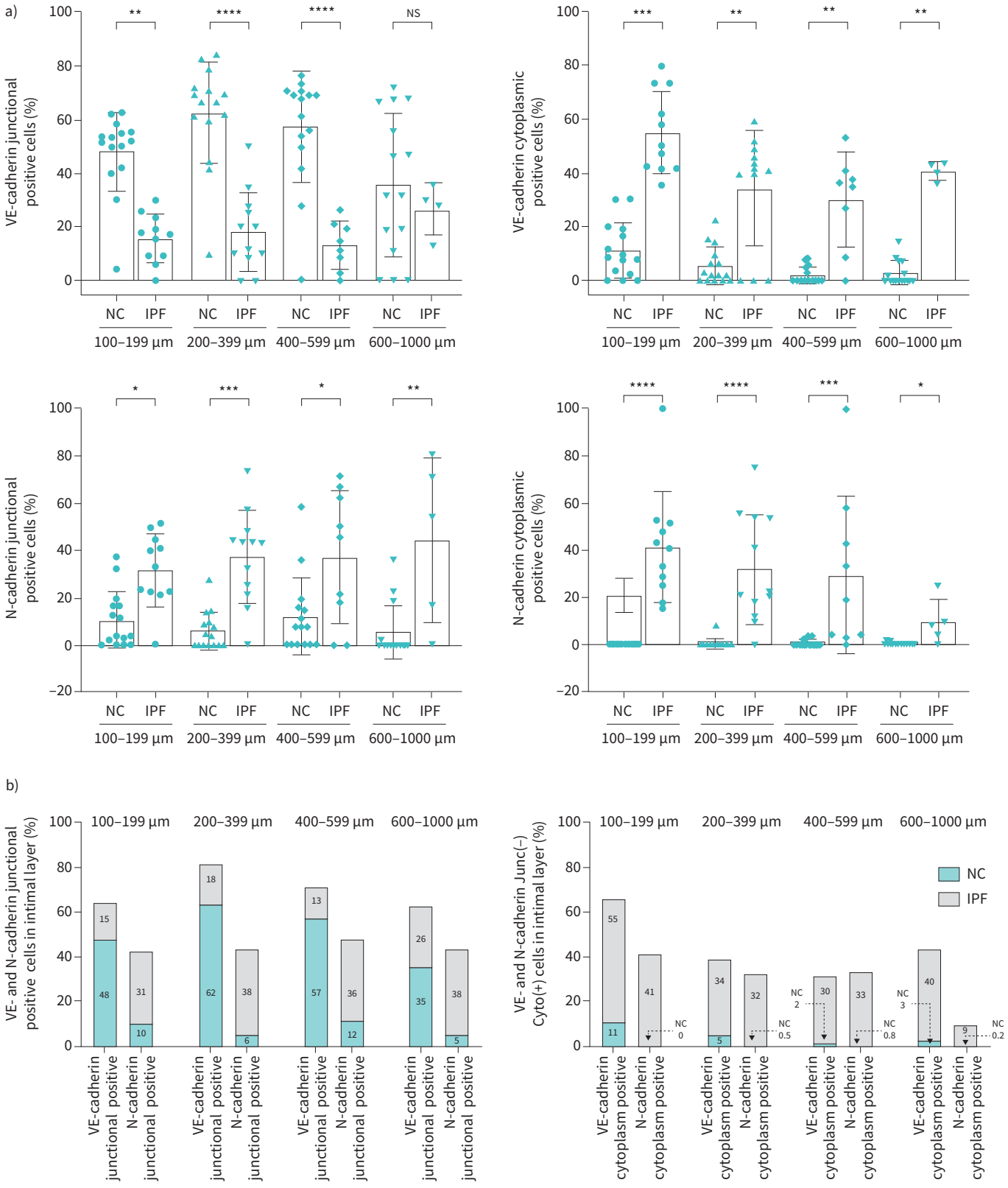


FIGURE 2 a) Per cent expression of VE-cadherin and N-cadherin positive cells in intimal layer in idiopathic pulmonary fibrosis (IPF) and normal control (NC) across arterial sizes 100–1000 µm: VE-cadherin junctional positive, VE-cadherin cytoplasmic positive, N-cadherin junctional positive and N-cadherin cytoplasmic positive. b) VE-cadherin and N-cadherin positive cells ratio in IPF and NC: VE-cadherin junctional positive *versus* N-cadherin junctional positive, and VE-cadherin cytoplasmic positive *versus* N-cadherin cytoplasmic positive. All data are presented as multiple comparisons with ordinary one-way ANOVA; p≤0.05 was considered significant. *p<0.05, **p<0.01, ***p<0.001, ****p<0.0001 was considered significant. NS: nonsignificant.

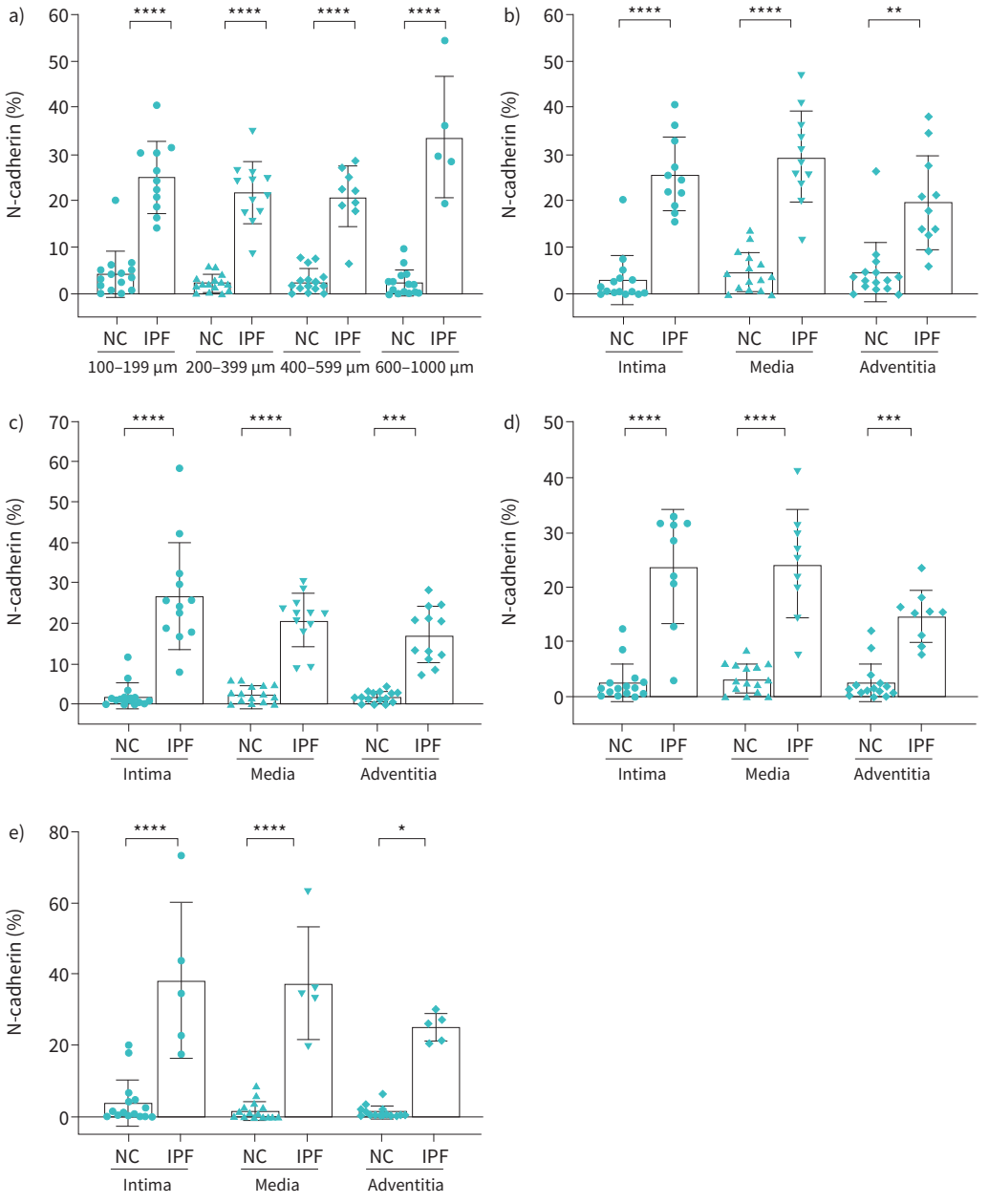


FIGURE 3 N-cadherin expression in normal control (NC) and idiopathic pulmonary fibrosis (IPF): a) total arterial N-cadherin expression across arterial sizes 100–1000 µm, b) 100–199 µm, c) 200–399 µm, d) 400–599 µm and e) 600–1000 µm. All data are presented as multiple comparisons with ordinary one-way ANOVA; $p \leq 0.05$ was considered significant. *p<0.05, **p<0.01, ***p<0.001, ****p<0.0001 was considered significant.

(p<0.0001; figure 5b) compared to medium-sized arteries of 200–599 µm (p<0.001; figure 5c, d) in IPF. The medial and adventitial S100A4 expression did not change across arterial sizes. Overall, the smaller arteries showed more significant changes in S100A4 expression compared to medium- and large-sized arteries (figure 5b, c, d, f).

### *Mesenchymal maker expression impacted vascular remodelling and lung physiology*

There was a significant positive correlation between increased total N-cadherin and arterial thickening (r′=058, p=0.03) (figure 6a). Total vimentin expression showed a positive association (r′=0.37, p=0.13) with increased arterial thickness (figure 6b). Remarkably, intimal N-cadherin and vimentin expression significantly positively corelated to both intimal (r′=0.64, p=0.01) and adventitial thickness (r′=0.63, p=0.03) (table 2). Total N-cadherin and vimentin expression also showed a significant negative correlation

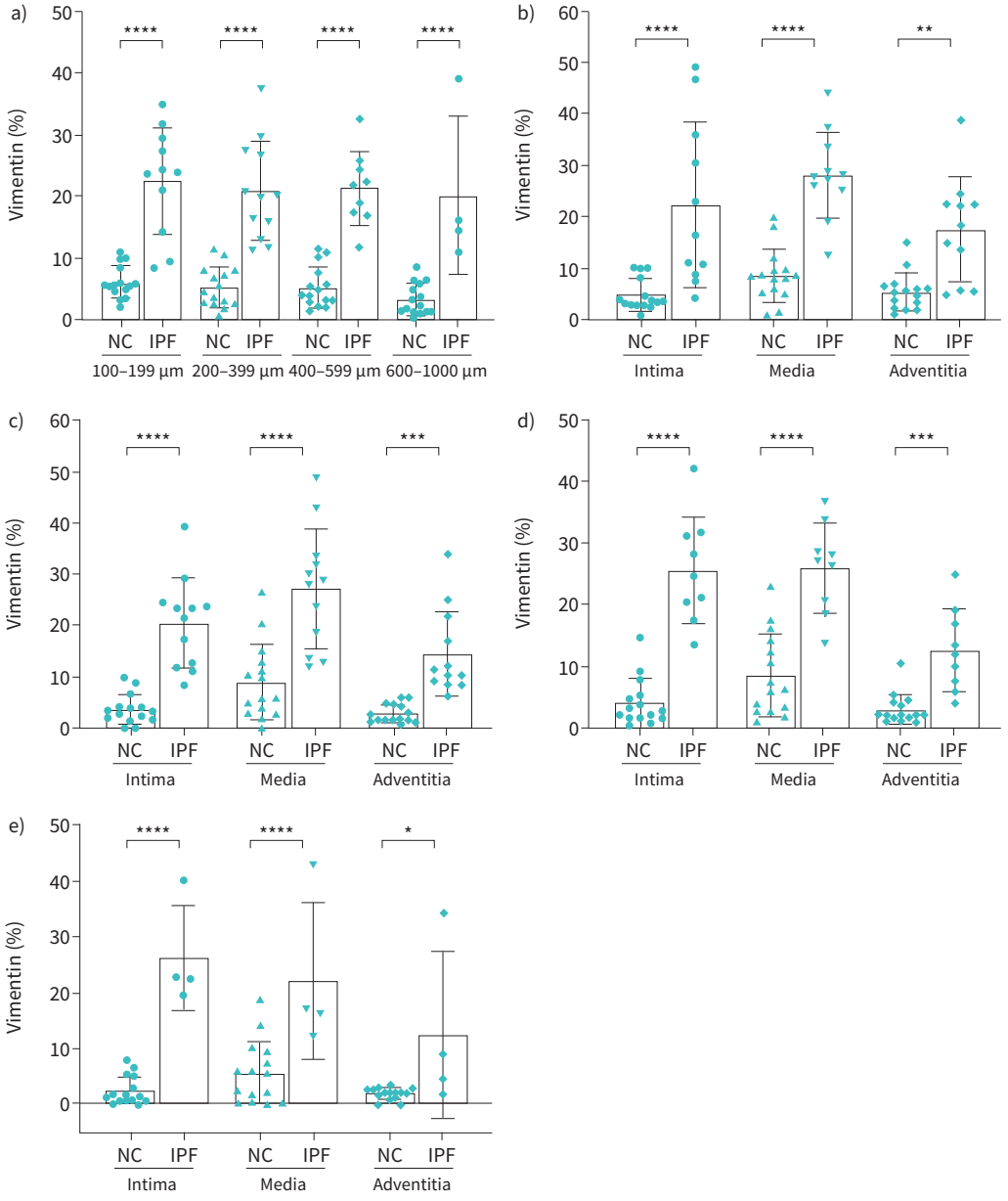


FIGURE 4 Vimentin expression in normal control (NC) and idiopathic pulmonary fibrosis (IPF): a) total arterial vimentin expression across arterial sizes 100–1000 µm, b) 100–199 µm, c) 200–399 µm, d) 400–599 µm and e) 600–1000 µm. All data are presented as multiple comparisons with ordinary one-way ANOVA; $p \leq 0.05$ was considered significant. *p<0.05, **p<0.01, ***p<0.001, ****p<0.0001 was considered significant.

with diffusing capacity of the lung for carbon monoxide ($D_{LCO}$) % predicted $r' = -0.66$, p=0.01 and $r' = -0.63$, p=0.03, respectively (figure 6c, d). We also noted that increases in intimal N-cadherin and vimentin negatively correlated to $D_{LCO}$ % predicted ($r' = -0.58$, p=0.03; table 2).

### *Correlation between intimal junctional and cytoplasmic VE-cadherin expression and mesenchymal proteins*

We identified an interesting relationship between junctional and cytoplasmic VE-cadherin expression and mesenchymal protein expression in the intimal layer across classified arteries. A negative correlation between VE-cadherin junctional and mesenchymal protein vimentin, N-cadherin and S100A4 was observed between smaller and larger arteries (supplementary figure S2a and d). However, the association between junctional VE-cadherin and intimal vimentin was significant in arteries of size 100–199 µm ($r' = -0.85$, p=0.001) (supplementary figure S2a), whereas a strong negative relationship was also seen in

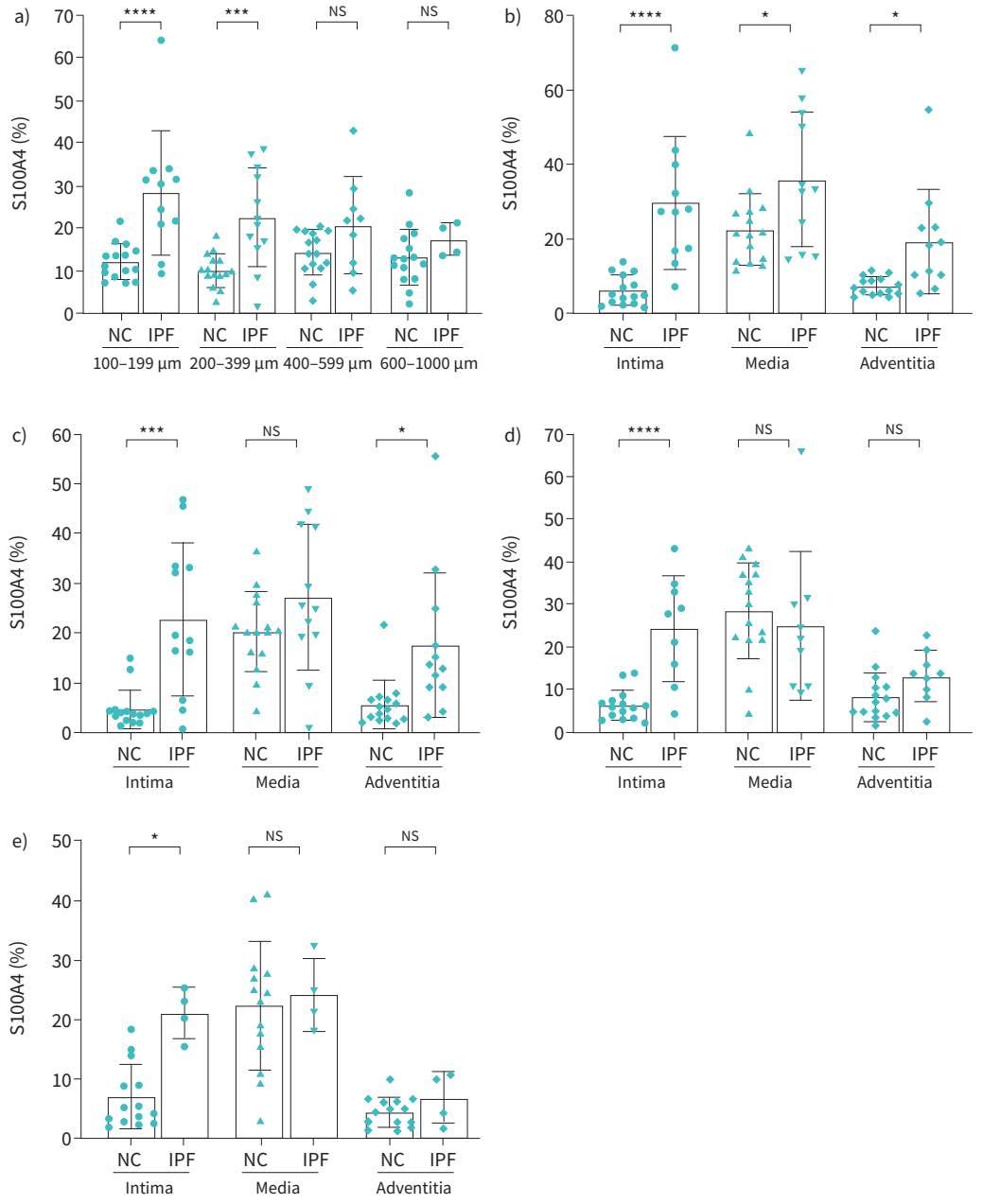


FIGURE 5 S100A4 expression in normal control (NC) and idiopathic pulmonary fibrosis (IPF): a) total arterial vimentin expression across arterial sizes 100–1000 µm, b) 100–199 µm, c) 200–399 µm, d) 400–599 µm and e) 600–1000 µm. All data are presented as multiple comparisons with ordinary one-way ANOVA; p≤0.05 was considered significant. *p<0.05, ***p<0.001, ****p<0.0001 was considered significant. NS: nonsignificant.

larger arteries of 600–1000 µm ($r' = -0.88$, p=0.31) (supplementary figure S2d). Furthermore, the association between junctional VE-cadherin and intimal S100A4 was also negative for all arterial sizes apart from 400–599 µm (supplementary figure S2a–d).

We also observed a consistent positive relationship trend between VE-cadherin cytoplasmic expression and intimal mesenchymal protein vimentin, N-cadherin and S100A4 in smaller and medium-sized arteries (supplementary figure S2a and b). However, we could not identify a comparable pattern in larger arterial sizes (supplementary figure S2c and d), which might be due to the high sample size variability observed between IPF and NCs.

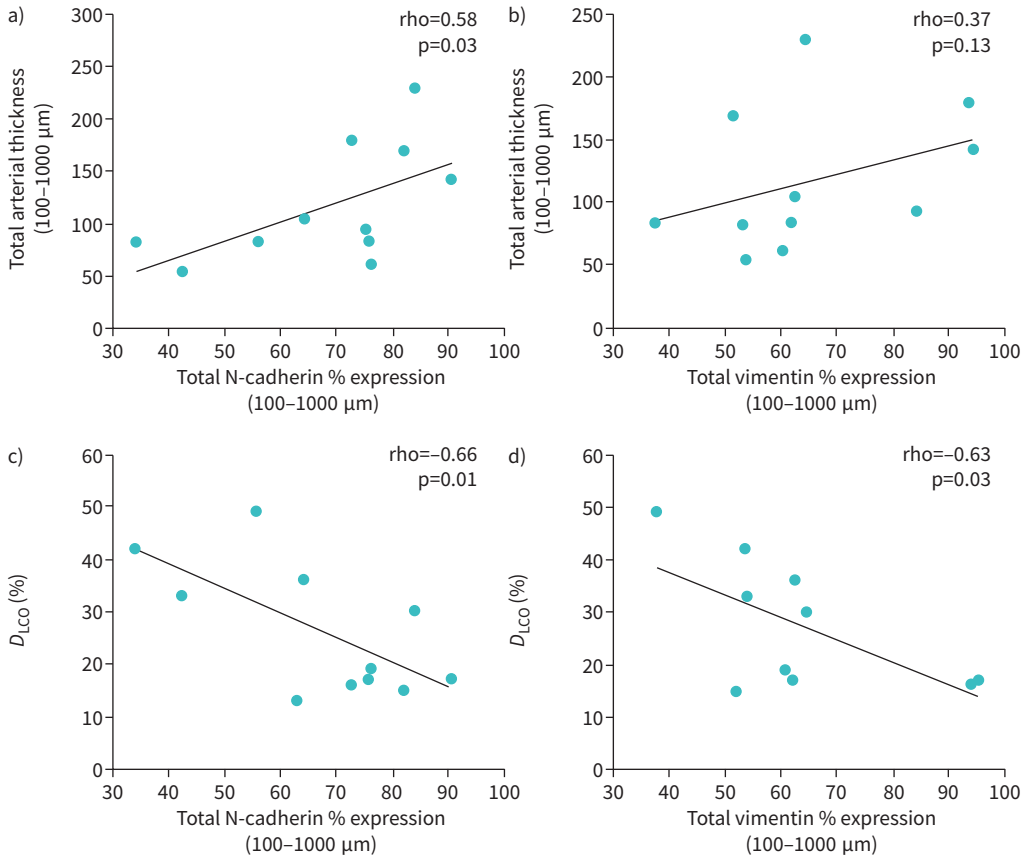


FIGURE 6 Correlations between a) total N-cadherin % expression *versus* total arterial thickness, b) total vimentin % expression *versus* total arterial thickness, c) total N-cadherin % expression *versus* % diffusing capacity of the lung for carbon monoxide ($D_{LCO}$) and d) total vimentin % expression *versus* % $D_{LCO}$.

### *CD4/CD8, mast cells, neutrophil, macrophage and pericyte cell expression in pulmonary arteries from patients with IPF compared to NCs*

We found negative expressions of CD4, CD8, neutrophil elastase and CMA1 for mast cells in the arterial wall of patients with IPF. CD68 (macrophage) was the only inflammatory cell type with positive staining,

TABLE 2 Correlation analysis of mesenchymal markers *versus* arterial thickness and lung function

| Correlation analysis | Intimal N-cadherin | Intimal vimentin |
|---|---|---|
| **Arterial thickness** | | |
| Intima | r′=0.64 | r′=0.60 |
| | p=0.01 | p=0.03 |
| Media | r′=0.12 | r′=0.10 |
| | p=0.36 | p=0.38 |
| Adventitia | r′=0.28 | r′=0.25 |
| | p=0.19 | p=0.22 |
| **Lung function** | | |
| $FEV_1$ L | r′= −0.40 | r′=0.05 |
| | p=0.09 | p=0.44 |
| FVC L | r′= −0.27 | r′=0.18 |
| | p=0.20 | p=0.29 |
| $D_{LCO}$ % | r′= −0.58 | r′= −0.56 |
| | p=0.04 | p=0.03 |

p⩽0.05 was considered significant. $FEV_1$: forced expiratory volume in 1 s; FVC: forced vital capacity; $D_{LCO}$: diffusing capacity of the lung for carbon monoxide.

but more so in the lumen of the artery or adventitial layer in IPF. Intimal endothelial cells were negative for CD68. In addition, we observed positive expression for PDGFR-β, which is a marker for pericytes. We found positive staining for pericytes in the intimal layer and the surrounding tissue, but endothelial cells were negative for this marker as shown in the inset in figure 7b. Staining for inflammatory markers and pericytes is shown in figure 7a and b.

## Discussion

This study, to the best of our knowledge, is the first description of EndMT in the arterial vasculature of patients with IPF. We have provided both qualitative and quantitative data informing EndMT marker expression across different arterial sizes and individual layers. Our study demonstrated downregulation of junctional VE-cadherin and increased cytoplasmic VE-cadherin in patients with IPF compared with NCs. Furthermore, we showed upregulation of the mesenchymal proteins N-cadherin, vimentin and S100A4 across classified arteries in IPF. The mesenchymal expression was most prominent within the intima, suggesting that endothelial transformation *via* EndMT is an active process in the pulmonary arteries of patients with IPF. Strong co-relations between EndMT and arterial remodelling were observed; these included arterial thickness and ECM deposition. Moreover, we found EndMT to adversely influence lung physiological parameters, especially $D_{LCO}$. Our findings suggest EndMT as a novel therapeutic target in IPF.

EndMT is a crucial process in developing and progressing fibrotic changes [10–12]. VE-cadherin is an endothelial cell-specific protein [20] that controls permeability and regulates cell motility [21]. Our study noted a significant reduction of VE-cadherin expression across all arterial sizes in IPF and a concurrent increase in cytoplasmic VE-cadherin at the intimal layer across all arterial sizes. Junctional to cytoplasmic VE-cadherin expression shift suggests that endothelial cell integrity is compromised in IPF favouring EndMT. Mammoto *et al.* [22] cultured human lung microvascular endothelial (L-HMVE) cells in fibronectin-coated polyacrylamide gels with different stiffness to investigate changes in mechanical interactions that could regulate vascular permeability. They observed that L-HMVE cells grown on more flexible substrates appeared round and VE-cadherin-containing cell–cell junctions were disrupted, and this was associated with increased VE-cadherin staining in the cytoplasm [22].

Further, parallel to VE-cadherin expression, we observed an increase in mesenchymal proteins vimentin, S100A4 and N-cadherin in the intimal layer of arteries. Previous IPF studies have detected loss of endothelial phenotypes and acquisition of mesenchymal phenotypes, but these were mainly animal studies [13, 23]. In addition, previous work has suggested that the proliferation of both endothelial and smooth muscle cells that undergo phenotypic changes *via* EndMT is linked to intimal remodelling and PH pathology [24]. Moreover, augmented mesenchymal protein expression noted in the medial and adventitial layer suggests resident cells may undergo mesenchymal phenotypic transformation.

N-cadherin is also expressed in mesenchymal cells, which promotes motility and invasion [25]. We also discovered the augmented expression of N-cadherin junctional positive and N-cadherin cytoplasmic positive cells in the intimal layer among IPF patients. Previously, upregulated N-cadherin expression in alveolar type II cells has been observed in IPF patients and is considered a potential prognostic indicator based on N-cadherin and Ki-67 expression correlation with histological disease activity [26]. Recently, Ferrell *et al*. [27] also demonstrated that retention of the N-cadherin prodomain at the cell surface is a potential biomarker of pathological myofibroblasts and is linked with fibrosis of tissues of the heart, lung and liver. Taken together, we believe that increase in cytoplasmic VE-cadherin could lead to the overall decrease in VE-cadherin and increase in N-cadherin indicating the process of EndMT, which drives intimal remodelling changes in IPF [1, 3]. Augmented mesenchymal protein expression noted in the medial and adventitial layer suggests resident cells may undergo mesenchymal phenotypic transformation.

The remodelling changes in medial and adventitial layers could be due to mesenchymal transformation of the smooth muscle cells and the adventitial fibroblast [28, 29]. N-cadherin was found to be abundantly expressed in both media and adventitia in IPF compared with the healthy control group. Moreover, the correlation between N-cadherin expression and vascular remodelling changes such as arterial thickness confirms increased N-cadherin expression is associated with increased individual layer thickness, especially intimal thickness. Thus, we suggest that targeting N-cadherin could be a potential strategy to reduce vascular remodelling, as suggested by earlier studies [30, 31].

Vimentin, a cytoskeletal protein that is prevalent in cells of mesenchymal origin, and its overexpression has been linked to increased invasiveness and excessive scarring [32]. Intriguingly, our study also discovered the augmented expression of vimentin at intimal, medial and adventitial layers for different arterial sizes in IPF. Several studies have noted vimentin overexpression in IPF lungs [33–37] with high

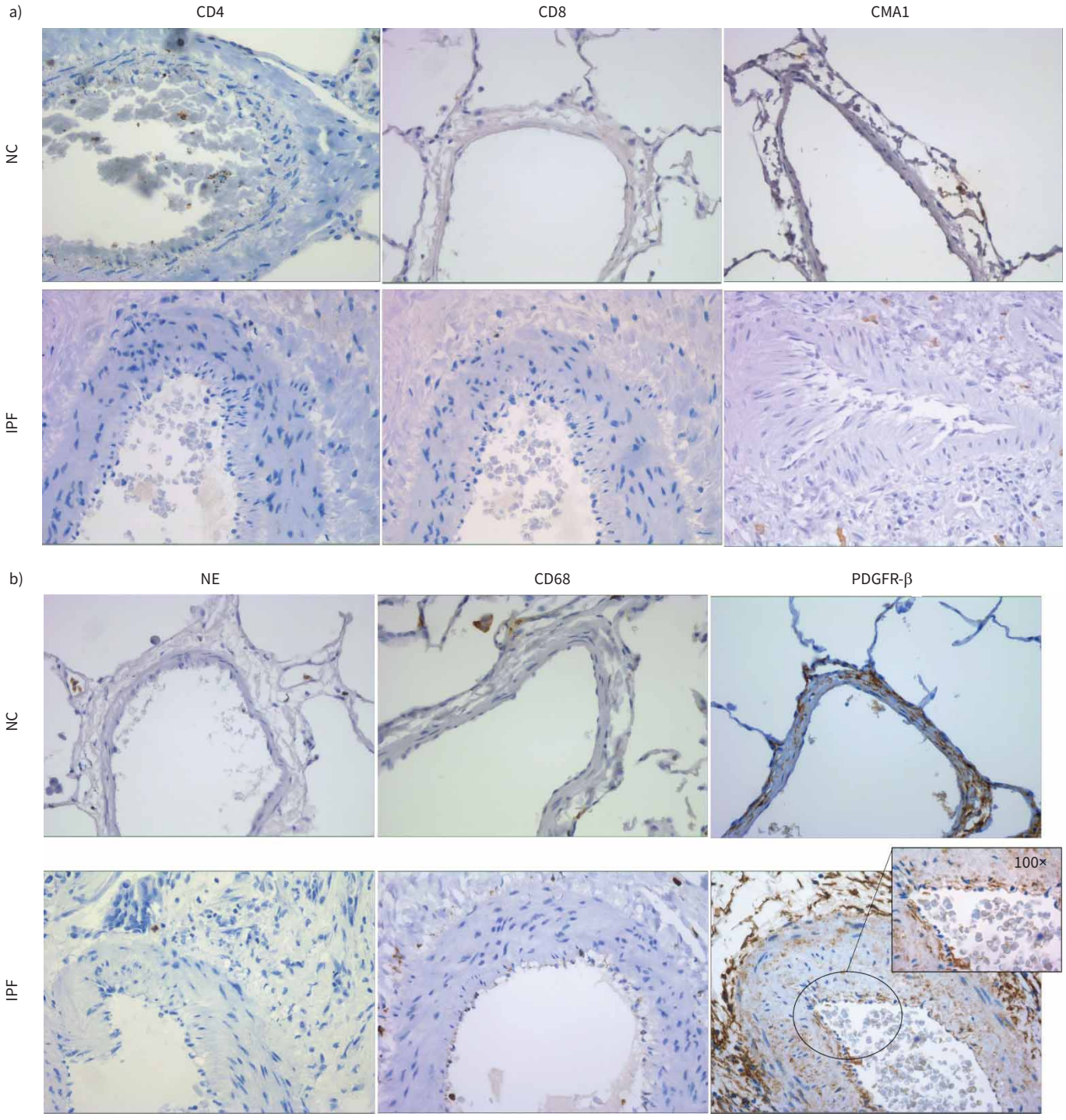


FIGURE 7 a) CD4, CD8 and mast cell chymase (CMA1) staining in arterial layers of normal control (NC) and patients with idiopathic pulmonary fibrosis (IPF). Images were taken at 40× magnification. b) Neutrophil elastase (NE), CD68 and PDGFR-β staining in arterial layers of NC and patients with IPF. Images were taken at 40× magnification, and the insert image was taken at 100× with a bright field.

levels of vimentin in IPF lung tissue related to disease progression [38]. Moreover, a positive correlation between total vimentin expression and arterial thickness suggests they play a role in arterial remodelling in IPF. Additionally, we observed that intimal vimentin expression influenced individual layer thickness, especially the intimal thickness.

S100A4 belongs to the small $Ca^{2+}$-binding protein family, and it modulates cellular biological functions, such as cell motility, proliferation and metastasis [39–41]. S100A4 causes lung fibrosis by promoting the proliferation and activation of fibroblasts [42–44], and increased S100A4 has been proposed to contribute to the development of IPF [45–48]. S100A4 expression was significantly higher in the intimal layer across all arterial sizes; however, we did not find such a significant expression in medial and adventitial layers.

We next investigated the relationship between VE-cadherin junctional and cytoplasmic positive expression and mesenchymal protein expression, which suggested that upregulated VE-cadherin cytoplasmic expression is associated with increased mesenchymal protein expression, especially in case of smaller and medium-sized arteries. However, larger arteries did not show similar changes, possibly due to the smaller number of larger arteries observed in fibrotic IPF lung tissue. This trend suggests increased cytoplasmic VE-cadherin expression in endothelial cells could indicate active endothelial proliferation and transition.

In assessing the impact of EndMT on lung function, a correlation between expression of mesenchymal markers and lung function parameter $D_{LCO}$ was performed. The correlations suggested that the increase in N-cadherin and vimentin expression could negatively impact lung gas exchange capacity ($D_{LCO}$) in IPF patients, indicating PH complications. Furthermore, the reduced $D_{LCO}$ in IPF patients has been considered as an indication of concomitant PH to the underlying pulmonary fibrosis [49]. Our findings fit with this theory and suggested pathology.

To further confirm our EndMT findings and cellular expression of mesenchymal markers, we also stained for inflammatory cell populations and pericytes. We found that pulmonary arteries were negative for mast cells, CD4/CD8 and neutrophils. Some positivity was observed for macrophages ($CD68^+$), but mainly in the lumen or adventitial tissue. Endothelial cells were negative for CD68. We also found positive staining for pericytes, but intimal endothelial cells were negative for PDGFR-β. This shows that endothelial cells staining for mesenchymal markers are not inflammatory cells but in fact the cells undergoing EndMT. Pericytes could also be contributing to arterial remodelling in IPF in addition to endothelial cells, but this warrants further work.

One limitation of this study is that the number of IPF and NC samples varied for size-based comparison, as some arterial sizes were not observed in IPF. Another limitation is the unavailability of cardiac function data or a clinical diagnosis of PH for the IPF patients studied; hence, the associations between EndMT and PH could not be established. However, the positive correlation of EndMT with vascular remodelling and negative correlation with $D_{LCO}$ indicates possible PH in IPF patients. Further work is needed to confirm these associations. Future studies are needed to further explore these histopathological findings with relationships to transcriptomics [50].

In summary, endothelial cells acquire mesenchymal traits through EndMT in IPF patients. Significant increased mesenchymal expression in arterial layers potentially contributes to remodelling of muscular arteries and drives physiological changes, such as deficient oxygen absorption. Hence, our study data validated the crucial role of EndMT in IPF pathology and suggest EndMT as a novel therapeutic target for preventing PH and lung fibrosis in general.

Provenance: Submitted article, peer reviewed.

Conflict of interest: S.S. Sohal reports personal fees for lectures from Chiesi, travel support from Chiesi and AstraZeneca, and a research grant from Boehringer Ingelheim outside the submitted work. S.S. Sohal is on the Small Airway Advisory Board for Chiesi Australia. All the other authors have no conflict of interest to declare.

Support statement: This work was supported by research grants from Clifford Craig Foundation Launceston General Hospital and Lung Foundation Australia. Funding information for this article has been deposited with the Crossref Funder Registry.

## References

1 Gaikwad AV, Eapen MS, McAlinden KD, *et al.* Endothelial to mesenchymal transition (EndMT) and vascular remodeling in pulmonary hypertension and idiopathic pulmonary fibrosis. *Expert Rev Respir Med* 2020; 14: 1027–1043.

2 Richeldi L, Collard HR, Jones MG. Idiopathic pulmonary fibrosis. *Lancet* 2017; 389: 1941–1952.

3 Gaikwad AV, Lu W, Dey S, *et al.* Vascular remodelling in IPF patients and its detrimental effect on lung physiology: potential role of endothelial to mesenchymal transition (EndMT). *ERJ Open Res* 2022; 8: 00571-02021.
4 Nathan SD, Shlobin OA, Ahmad S, *et al.* Serial development of pulmonary hypertension in patients with idiopathic pulmonary fibrosis. *Respiration* 2008; 76: 288–294.
5 Farkas L, Gauldie J, Voelkel NF, *et al.* Pulmonary hypertension and idiopathic pulmonary fibrosis: a tale of angiogenesis, apoptosis, and growth factors. *Am J Respir Cell Mol Biol* 2011; 45: 1–15.
6 Nathan SD, Barbera JA, Gaine SP, *et al.* Pulmonary hypertension in chronic lung disease and hypoxia. *Eur Respir J* 2019; 53: 1801914.
7 Lettieri CJ, Nathan SD, Barnett SD, *et al.* Prevalence and outcomes of pulmonary arterial hypertension in advanced idiopathic pulmonary fibrosis. *Chest* 2006; 129: 746–752.
8 Kinoshita T, Goto T. Molecular mechanisms of pulmonary fibrogenesis and its progression to lung cancer: a review. *Int J Mol Sci* 2019; 20: 1461.
9 Wynn TA. Integrating mechanisms of pulmonary fibrosis. *J Exp Med* 2011; 208: 1339–1350.
10 Ursoli Ferreira F, Eduardo Botelho Souza L, Hassibe Thomé C, *et al.* Endothelial cells tissue-specific origins affects their responsiveness to TGF-β2 during endothelial-to-mesenchymal transition. *Int J Mol Sci* 2019; 20: 458.
11 Lv Z, Wang Y, Liu Y-J, *et al.* NLRP3 inflammasome activation contributes to mechanical stretch–induced endothelial-mesenchymal transition and pulmonary fibrosis. *Crit Care Med* 2018; 46: e49–e58.
12 Piera-Velazquez S, Mendoza FA, Jimenez SA. Endothelial to mesenchymal transition (EndoMT) in the pathogenesis of human fibrotic diseases. *J Clin Med* 2016; 5: 45.
13 Hashimoto N, Phan SH, Imaizumi K, *et al.* Endothelial–mesenchymal transition in bleomycin-induced pulmonary fibrosis. *Am J Respir Cell Mol Biol* 2010; 43: 161–172.
14 Choi SH, Hong ZY, Nam JK, *et al.* A hypoxia-induced vascular endothelial-to-mesenchymal transition in development of radiation-induced pulmonary fibrosis. *Clin Cancer Res* 2015; 21: 3716–3726.
15 Rieder F, Kessler SP, West GA, *et al.* Inflammation-induced endothelial-to-mesenchymal transition: a novel mechanism of intestinal fibrosis. *Am J Pathol* 2011; 179: 2660–2673.
16 Yoshimatsu Y, Watabe T. Roles of TGF-β signals in endothelial-mesenchymal transition during cardiac fibrosis. *Int J Inflam* 2011; 2011: 724080.
17 Eapen MS, Lu W, Gaikwad AV, *et al.* Endothelial to mesenchymal transition: a precursor to post-COVID-19 interstitial pulmonary fibrosis and vascular obliteration? *Eur Respir J* 2020; 56: 2003167.
18 Sanchez-Duffhues G, Orlova V, ten Dijke P. In Brief: Endothelial-to-mesenchymal transition. *J Pathol* 2016; 238: 378–380.
19 Bhattarai P, Lu W, Gaikwad AV, *et al.* Arterial remodelling in smokers and in patients with small airway disease and COPD: implications for lung physiology and early origins of pulmonary hypertension. *ERJ Open Res* 2022; 8: 00254-2022.
20 Ampugnani MG, Resnati M, Raiteri M, *et al.* A novel endothelial-specific membrane protein is a marker of cell-cell contacts. *J Cell Biol* 1992; 118: 1511–1522.
21 Vestweber D, Winderlich M, Cagna G, *et al.* Cell adhesion dynamics at endothelial junctions: VE-cadherin as a major player. *Trends Cell Biol* 2009; 19: 8–15.
22 Mammoto A, Mammoto T, Kanapathipillai M, *et al.* Control of lung vascular permeability and endotoxin-induced pulmonary oedema by changes in extracellular matrix mechanics. *Nat Commun* 2013; 4: 1759.
23 Jia W, Wang Z, Gao C, *et al.* Trajectory modeling of endothelial-to-mesenchymal transition reveals galectin-3 as a mediator in pulmonary fibrosis. *Cell Death Dis* 2021; 12: 327.
24 Ghigna M-R, Dorfmüller P. Pulmonary vascular disease and pulmonary hypertension. *Diagn Histopathol* 2019; 25: 304–312.
25 Wheelock MJ, Johnson KR. Cadherins as modulators of cellular phenotype. *Annu Rev Cell Dev Biol* 2003; 19: 207–235.
26 Lomas NJ, Watts KL, Akram KM, *et al.* Idiopathic pulmonary fibrosis: immunohistochemical analysis provides fresh insights into lung tissue remodelling with implications for novel prognostic markers. *Int J Clin Exp Pathol* 2012; 5: 58–71.
27 Ferrell PD, Oristian KM, Cockrell E, *et al.* Pathologic proteolytic processing of N-cadherin as a marker of human fibrotic disease. *Cells* 2022; 11: 156.
28 Kuwabara JT, Tallquist MD. Tracking adventitial fibroblast contribution to disease: a review of current methods to identify resident fibroblasts. *Arterioscler Thromb Vasc Biol* 2017; 37: 1598–1607.
29 Stenmark KR, Davie N, Frid M, *et al.* Role of the adventitia in pulmonary vascular remodeling. *Physiology (Bethesda)* 2006; 21: 134–145.
30 Jones M, Sabatini PJB, Lee FSH, *et al.* N-Cadherin upregulation and function in response of smooth muscle cells to arterial injury. *Arterioscler Thromb Vasc Biol* 2002; 22: 1972–1977.
31 Lyon CA, Koutsouki E, Aguilera CM, *et al.* Inhibition of N-cadherin retards smooth muscle cell migration and intimal thickening via induction of apoptosis. *J Vasc Surg* 2010; 52: 1301–1309.
32 Li H, Chang L, Du WW, *et al.* Anti-microRNA-378a enhances wound healing process by upregulating integrin beta-3 and vimentin. *Mol Ther* 2014; 22: 1839–1850.

33 Yang Y, Fujita J, Bandoh S, *et al.* Detection of antivimentin antibody in sera of patients with idiopathic pulmonary fibrosis and non-specific interstitial pneumonia. *Clin Exp Immunol* 2002; 128: 169–174.
34 Felton VM, Borok Z, Willis BC. N-acetylcysteine inhibits alveolar epithelial-mesenchymal transition. *Am J Physiol Lung Cell Mol Physiol* 2009; 297: L805–L812.
35 Pandit KV, Corcoran D, Yousef H, *et al.* Inhibition and role of let-7d in idiopathic pulmonary fibrosis. *Am J Respir Crit Care Med* 2010; 182: 220–229.
36 Liu G, Philp AM, Corte T, *et al.* Therapeutic targets in lung tissue remodelling and fibrosis. *Pharmacol Ther* 2021; 225: 107839.
37 Zhang D, Zhuang R, Li J, *et al.* MicroSPECT imaging-guided treatment of idiopathic pulmonary fibrosis in mice with a vimentin-targeting 99mTc-labeled N-acetylglucosamine-polyethyleneimine. *Mol Pharm* 2021; 18: 4140–4147.
38 Surolia R, Li FJ, Wang Z, *et al.* Vimentin intermediate filament assembly regulates fibroblast invasion in fibrogenic lung injury. *JCI Insight* 2019; 4: e123253.
39 Grigorian M, Andresen S, Tulchinsky E, *et al.* Tumor suppressor p53 protein is a new target for the metastasis-associated Mts1/S100A4 protein: functional consequences of their interaction. *J Biol Chem* 2001; 276: 22699–22708.
40 Boye K, Mælandsmo GM. S100A4 and metastasis: a small actor playing many roles. *Am J Pathol* 2010; 176: 528–535.
41 Li Z-H, Bresnick AR. The S100A4 metastasis factor regulates cellular motility via a direct interaction with myosin-IIA. *Cancer Res* 2006; 66: 5173–5180.
42 Xia H, Gilbertsen A, Herrera J, *et al.* Calcium-binding protein S100A4 confers mesenchymal progenitor cell fibrogenicity in idiopathic pulmonary fibrosis. *J Clin Invest* 2017; 127: 2586–2597.
43 Li Y, Bao J, Bian Y, *et al.* S100A4(+) macrophages are necessary for pulmonary fibrosis by activating lung fibroblasts. *Front Immunol* 2018; 9: 1776.
44 Zhang W, Ohno S, Steer B, *et al.* S100a4 is secreted by alternatively activated alveolar macrophages and promotes activation of lung fibroblasts in pulmonary fibrosis. *Front Immunol* 2018; 9: 1216.
45 Lee J-U, Chang HS, Shim E-Y, *et al.* The S100 calcium-binding protein A4 level is elevated in the lungs of patients with idiopathic pulmonary fibrosis. *Respir Med* 2020; 171: 105945.
46 Li Z, Li Y, Liu S, *et al.* Extracellular S100A4 as a key player in fibrotic diseases. *J Cell Mol Med* 2020; 24: 5973–5983.
47 Kagimoto A, Tsutani Y, Kushitani K, *et al.* Serum S100 calcium-binding protein A4 as a novel predictive marker of acute exacerbation of interstitial pneumonia after surgery for lung cancer. *BMC Pulm Med* 2021; 21: 186.
48 Qin H-Y, Li M-D, Xie G-F, *et al.* Associations among S100A4, Sphingosine-1–Phosphate, and pulmonary function in patients with chronic obstructive pulmonary disease. *Oxid Med Cell Longev* 2022; 2022: 6041471.
49 Ruffenach G, Hong J, Vaillancourt M, *et al.* Pulmonary hypertension secondary to pulmonary fibrosis: clinical data, histopathology and molecular insights. *Respir Res* 2020; 21: 303.
50 Ackermann M, Stark H, Neubert L, *et al.* Morphomolecular motifs of pulmonary neoangiogenesis in interstitial lung diseases. *Eur Respir J* 2020; 55: 1900933.